Bifurcation and chaos phenomena appearing in induction motor under variation of PI controller parameters

N. JABLI [1], H. KHAMMARI [2], M.F. MIMOUNI [1] and R. DHIFAOUI [3]
(1) National Engineering School of Monastir
Ibn aljazar street, 5019 Monastir, Tunisia
jabli.nizar@yahoo.fr ; mfaouzi.mimouni@enim.rnu.tn
(2) College of Computer Science and Information Systems
Taif University, Arabi saoudi
gham.hedi@hotmail.com
(3) National Institute of Applied Sciences and Technology
North Urban Center, B.P 676, 1080 Tunis Cedex, Tunisa.
Rachid.Dhifaoui@insat.rnu.tn

Abstract: Bifurcation theory deals with the change of qualitative behavior in a parameter space of dynamical systems. This paper provides a numerical approach to better understand the dynamic behavior of an indirect field oriented control (IFOC) of a current-fed induction motor. The focus is on bifurcation analysis of the IFOC motor model parameters, with a particular emphasis on the change that affects the dynamics and stability under small variations of Proportional Integral controller (PI) parameters. In fact, the dynamical properties of this electrical machine exhibit a rich behavior. Indeed equilibrium point and complex oscillatory phenomena such as limit cycle and chaos are observed. Since a perturbation of PI control gains led to the existence of regular behavior and region where chaotic phenomena may occur. Properties of both parametric and phase plane singularities are carried out by using numerical simulations. Furthermore, bifurcation diagrams for the equilibrium points and the 2-parametric bifurcation curves are computed based on continuation methods for solving differential equations. This paper also attempts to discuss various types of the transition to chaos in the induction motor model. The analysis of the obtained bifurcation simulations gives useful guidelines for adjusting both motor model and PI controller parameters.

Key–Words: Induction motor, PI Controller gains, Qualitative behavior, Bifurcation, Chaos.

1 Introduction

The application of bifurcation theory to areas outside of mathematics is currently a field of active research. This theory has recently spread to various and interdisciplinary domains including physics, biology, mechanical and electrical engineering. The aim of bifurcation theory is that its analysis methods make essentially possible to qualitatively discuss about the behavior of a nonlinear dynamical system at close to critical values of control parameters called also singular points. Generally, nonlinear dynamical systems undergo abrupt qualitative changes when crossing bifurcation points. For a more exhaustive investigation of mechanism responses of such nonlinear dynamic system it is compulsory to identify both singularities of the parameter plane (bifurcation points, chaos, ...) and singularities of the phase plane (fixed or equilibrium points, cycles, invariant closed curves, ...) [1],[2].

Recently, a highly interesting consideration has been conducted by design engineers to the results derived from a qualitative investigation of real systems such as electrical circuits and machines. In particular, qualitative bifurcation analysis has since been successfully employed as a useful tool to better understand the dynamical behavior of induction motors [3], [4],[5]. Generally, bifurcation phenomenon is a dynamic behavior associated with loss of stability. At the bifurcation point, multistability propriety can be detected, i.e. existence and uniqueness of solutions is not guaranteed and a change in the number of solutions occurs.

Frequently, the field-oriented controllers (FOC) is used as nonlinear controllers to achieve high dynamic performance in induction machines. This

technique performs asymptotic linearization and decoupling [6]. Stability of FOC is generally investigated regarding errors in the estimate of the rotor resistance. An analysis of saddle-node and Hopf bifurcations in indirect field-oriented control (IFOC) drives due to errors in the estimate of the rotor time constant provides a guideline for setting the gains of PI speed controller in order to avoid Hopf bifurcation [7]. An appropriate setting of the PI speed loop controller permits to keep the bifurcations far enough from the operating conditions in the parameter space [8]. It has been proven the occurrence of either codimension one bifurcation such as saddle node bifurcation and Hopf bifurcation and codimension two such as Bogdanov-Takens or zero-Hopf bifurcation in IFOC induction motors [9],[10],[11]. Other studies were concerned with the cancelation of sustained oscillations which are, in general undesirable. Some of such studies proposed an 'oscillation killer' method dedicated to control machine parameters in order to get rid of limit cycles [12]. In [13], chaotic rotation can promote efficiency or improve dynamic characteristics of drives. An adequate combination between analytical and numerical tools may provide a deep understanding of some nontrivial dynamical behavior related to bifurcation phenomena in a self-sustained oscillator [14]. The robustness margins for IFOC of induction motors can be deduced from the analysis of the bifurcation structures identified in parameter plane [15], [16]. Since the self-sustained oscillations in IFOC for induction motors may be due to the appearance of Hopf and Double Hopf bifurcation [17],[18]. An exhaustive study of the bifurcation structures is mainly devoted to preserve the local stability of the desired equilibrium point.
The aim of this work is to discuss some basic results regarding the qualitative study of the dynamic behavior of an IFOC induction motor where a PI controller takes place, with particular reference to bifurcation analysis. More importantly, we investigate the influence of PI controller parameters on the bifurcation scenarios under a small variation of its gains. In the literature such scenarios have not received much attention so far. The remainder of the paper is effectively split into three parts. The section 2 contains a brief description of electrical model of IFOC induction model. Basic remainders are then obtained in Section 3. In second part, section 4 presents multistability propriety in the IFOC induction motor. Finally, the remaining part of the paper concentrates simulations results on the study of the model: In Section 5, the bifurcation scenario under small variation of both parameters motor and PI controller gains are discussed, and Section 6 is devoted to study some cases of chaos detection in the model equations.

2 Equations model

In this section we consider the electrical model of an indirect field oriented control (IFOC) of a current-fed induction motor. A proportional-integral controller (PI) is employed in this model to act on the control of stator current input (i_{sq}).

$$i_{sq} = k_p\omega_e + k_i \int_0^t \omega_e(\theta)d\theta \tag{1}$$

The set of differential equations that describe the dynamics of motor with a null friction coefficient can be formulated in the following form:

$$\begin{aligned}
\dot{\varphi_{rd}} &= -\frac{1}{\tau_r}\varphi_{rd} + \frac{k}{\tau_r \, . \, i_{sd}^*}\varphi_{rq} i_{sq} + \frac{L_m}{\tau_r} i_{sd}^* && (2)\\
\dot{\varphi_{rq}} &= -\frac{1}{\tau_r}\varphi_{rq} + \frac{k}{\tau_r \, . \, i_{sd}^*}\varphi_{rd} i_{sq} + \frac{L_m}{\tau_r} i_{sq} && (3)\\
\dot{\omega_e} &= -\frac{n_p}{J}[\delta(\varphi_{rd} i_{sq} - \varphi_{rq} i_{sd}^*) - T_L] && (4)\\
\dot{i_{sq}} &= -k_p\frac{n_p}{J}[\delta(\varphi_{rd} i_{sq} - \varphi_{rq} i_{sd}^*) - T_L] + k_i\omega_e && (5)
\end{aligned}$$

where φ_{rd} and φ_{rq} stand for the direct and quadrature axis components of the rotor flux, respectively. The state variable $\omega_e = \omega_{ref} - \omega$ represents the difference between the reference and the real mechanical rotor speeds. $\tau_r = L_r/R_r$ being the rotor flux time constant. L_m denote the mutual inductance and L_r the rotor inductance, whereas R_r stand for the resistance in the rotor. J is the moment of inertia and n_p is the pole pair number. The parameter $k = \tau_r/\tau_e$, the ratio of the rotor time constant τ_r to its estimate τ_e and $i_{sd}^* = u_1^0$ is a design parameter. Finally, T_L is the load torque.
In the next sections we introduce the following notations of the state vector variable: $(\varphi_{rd}, \varphi_{rq}, \omega_e, i_{sq}) = (x_1, x_2, x_3, x_4)$.

3 General reminders

An autonomous system is generally described by a system of ordinary differential equations (ODEs) of the form:

$$\frac{dX}{dt} = f(X, \lambda);\ t \in IR,\ X \in IR^n,\ \lambda \in IR^p \tag{6}$$

where f is smooth. A bifurcation occurs at parameter $\lambda = \lambda_0$ if, crossing this value, the system behaviour undergo an abrupt change affecting the number or stability of equilibria or periodic orbits of f. As mentioned in previous papers [19], a two-parameter plane can be considered as made up of sheets (foliated representation), each one being associated with a well defined behaviour such as a fixed point, or an equilibrium or a periodic orbit.

Generally, the equation (6) can present multiple attractors as a single parameter varies. A local bifurcation at an equilibrium happens when some eigenvalues of the parameterized linear approximating differential equation cross some critical values such us the origin or the imaginary axis. Self-sustained oscillations in IFOC of induction motors can be originated by a codimension one bifurcation namely the Hopf bifurcation (H). Such kind of bifurcation can be computed from differential system(6), when a pair of complex conjugate eigenvalues among the eigenvalues set of the associate linearized system change from negative to positive real parts or vice versa. Therefore the Hopf bifurcation results from the transversal crossing of the imaginary axis by the pair of complex conjugate eigenvalues. Such bifurcation is said to be supercritical if the periodic branch is initially stable and subcritical if the periodic branch is initially unstable. The singularities of the phase plane are the solutions of 4th order autonomous ODEs describing the IFOC induction motor (Equilibrium points, limit cycles, chaotic orbits,...), each solution involves four eigenvalues describing its stability. A Saddle-node bifurcation (Fold (F)), or a limit point (LP)is a codimension one bifurcation which occurs when a single eigenvalue is equal to zero.

Some codimension two bifurcation points are considered in this paper such as the cuspidal point (CP), the Bogdanov-Taken bifurcation (BT) and the Generalized Hopf bifurcation (GH).
In a two parameter plane, a Bogdanov-Takens bifurcation happens for the assumption of an algebraically double zero eigenvalue, therefore, in a (k,T_L)-plane , a Bogdanov-Takens (BT) bifurcation occurs when an equilibrium point has a zero eigenvalue of multiplicity two. In the neighborhood of such bifurcation point, the system has at most two equilibria (a saddle and a non saddle) and a limit cycle. The limit cycle results from a non saddle equilibrium which undergoes an Andronov-Hopf bifurcation. Numerically, the normal Lyapunov exponents calculated in the Hopf bifurcation point are negative which means that these periodic orbits are born stable [20]. The saddle and nonsaddle equilibrium collide and disappear via a saddle-node bifurcation. This cycle degenerates into an orbit homoclinic to the saddle and disappears via a saddle homoclinic bifurcation.

A generalized Hopf (GH) bifurcation or Bautin bifurcation appears when a critical equilibrium has a pair of purely imaginary eigenvalues. The singular curves of the parameter plane corresponding to codimension-1 bifurcations may contain singular points of higher codimension. The simplest one located on a fold curve has the codimension-2, a *fold cusp*. It is the meeting point of two fold arcs. A Bogdanov-Taken bifurcation point (BT) will be identified on a saddle-node bifurcation curve, and a generalized Hopf bifurcation (GH) on a Hopf bifurcation curve.

4 Detection of multistability propriety

It is becoming increasingly clear that multistability is a major property of non linear dynamical systems and means the coexistence of more than one stable behavior for the same parameters set and for different initial conditions. Solving the differential system equation of IFOC model, the trajectory in state space will head for some final attracting region, or regions, which might be a point, curve, area, and so on. Such an object is called the attractor for the system. For the parameters $k = 4, kp = .4, ki = 1$ and $T_L = 0.5$, two different equilibrium points are identified :The first one is $(x^*_{10}, x^*_{20}, x^*_{30}, x^*_{40}) = (0.2764, -0.1383, 0, 1.309)$, solution of the differential system (2) for the initial conditions set $(x_{10}, x_{20}, x_{30}, x_{40}) = (1, 1, 0.1, 0.1)$ whereas $(x^*_{10}, x^*_{20}, x^*_{30}, x^*_{40}) = (0.7236, -0.3618, 0, 0.191)$ is the second one, and similarly a solution of (2) for the following initial conditions set $(x_{10}, x_{20}, x_{30}, x_{40}) = (1, -1, 0.1, 0.1)$. The phase trajectories converging to equilibrium points are given in both of phase planes (x_1, x_2) and (x_3, x_4) see figures 1 and 2. In figure 3 both of the red and the blue limit cycles coexist for the the parameters $k = 0.02017$; $kp = 0.15$; $ki = 1.01$ and $T_L = 10.1$, but for different initial conditions sets $(x_{10}, x_{20}, x_{30}, x_{40}) = (0.19, 0.5, 0, 0)$ and $(x_{10}, x_{20}, x_{30}, x_{40}) = (2.2, 7.5, 0.5, 7.5)$ respectively.

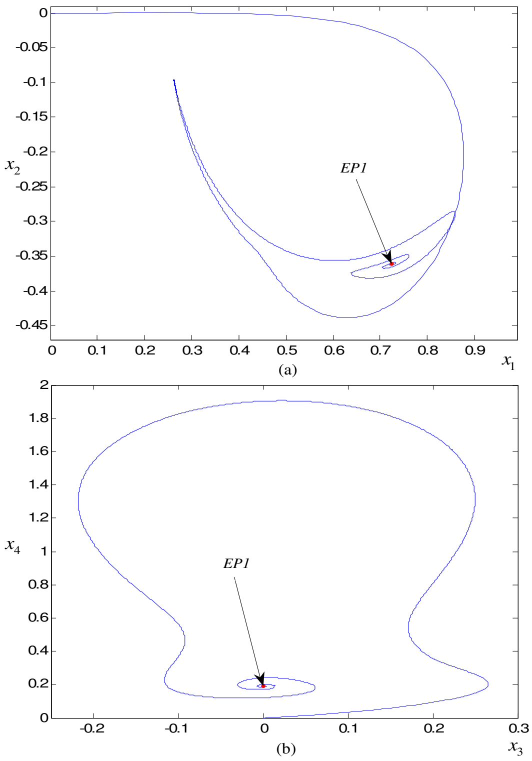

Figure 1: Equilibrium Point EP1 in phase planes (x_1, x_2) and (x_3, x_4)

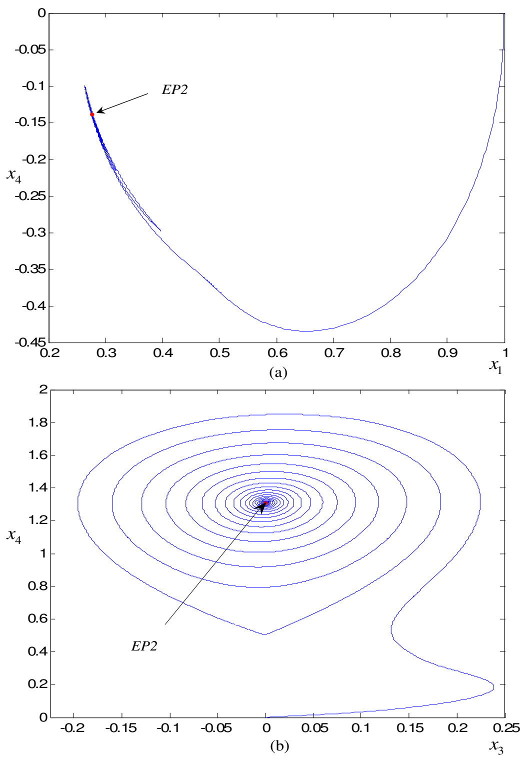

Figure 2: Equilibrium Point EP2 in phase planes (x_1, x_2) and (x_3, x_4)

5 Numerical computation of bifurcations sets

5.1 Hopf bifurcation detection

The detection of Hopf bifurcations in IFOC of induction motor is analyzed in both cases, zero load torque value ($T_L = 0$) and full load torque value ($T_L = 10$). for these two cases, phase trajectories undergo important qualitative changes under the variation of the parameter k. In the case of a load torque value $T_L = 0$, and $k = 1.65$, figure 4.a shows an equilibrium point illustrated by two phase trajectories in phase planes (x_1, x_2) and (x_3, x_4). However, for $k = 1.8$ the equilibrium point disappears and a limit cycle appears instead of it see figure 4.b. One can guess the existence of a Hopf bifurcation for $1.65 < k < 1.8$ which can be preciously computed using an adequate continuation program. For a load torque value $T_L = 10$, and for $k = 0.1$, figure 5.a presents a limit cycle illustrated by two closed trajectories in phase planes (x_1, x_2) and (x_3, x_4). Then for $k = 0.18$ the limit cycle disappears and an equilibrium point occurs instead of it see figure 5.b. One can guess the existence of a Hopf bifurcation for $0.17 < k < 0.18$. The Hopf bifurcation phenomenon, being one of the possible reasons for the oscillatory behavior, is an abrupt qualitative change that can be accompanied by a 'quantitative' change namely the spectral reorganization of the oscillating state variables. For example, an oscillatory regime is detected for the following parameter set $k = .1$, $kp = .1, ki = 1$ and $T_L = 10$. The figure 6.(b) and 6.(c) show the direct and quadratic fluxes waveform, respectively, under the above parameter values. The corresponding phase trajectory is shown in the figure 6.(a), which illustrate the periodic nature of system. The spectral analysis of periodic solutions, by means of Fourier Transform, was employed in [19] to characterize a succession of saddle-node bifurcation in a two parameter plane. Thus, the spectral approach applied to periodic solutions in nonautonomous systems may be extended to limit cycles in autonomous case.

5.2 Limit point and Hopf bifurcation points

Starting from a located initial equilibrium or a periodic orbit,numerical continuation is devoted to follow such special behavior as a single active

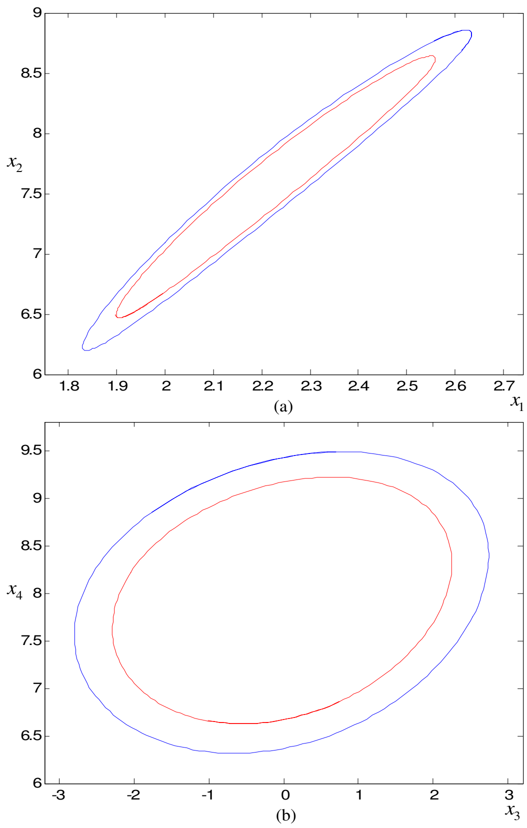

Figure 3: Limit cycles LC1 and LC2 in :
(a) phase plane (x_1, x_2) ,(b) phase plane (x_3, x_4)

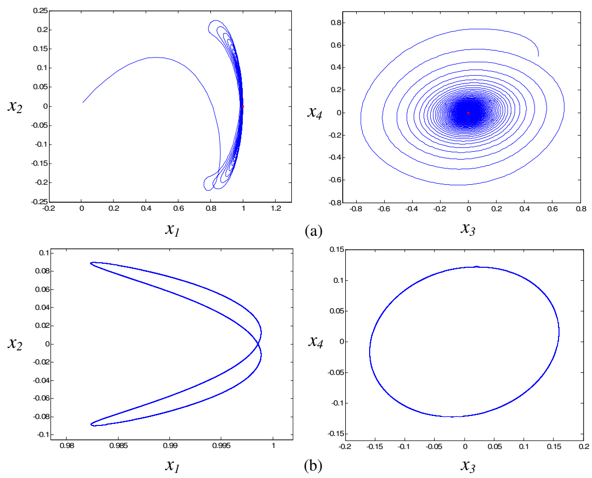

Figure 4: Hopf Bifurcation :phase trajectories in phase planes (x_1, x_2) and (x_3, x_4). for $kp = .1, ki = 1$ and $T_L = 10$. (a)$k = 1.65$,(b)$k = 1.8$.

parameter varies. The starting point is an equilibrium point
$(x^*_{10}, x^*_{20}, x^*_{30}, x^*_{40})$=(0.2764,-0.1383,0,1.309) computed for the parameters $k = 4, kp = .4, ki = 1$

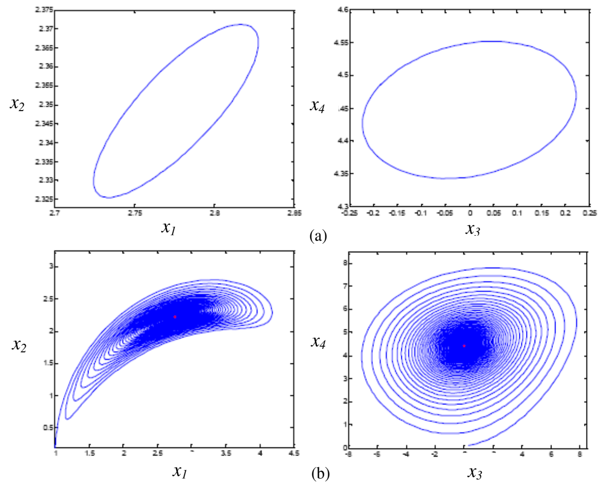

Figure 5: Hopf Bifurcation :phase trajectories in phase planes (x_1, x_2) and (x_3, x_4). for $kp = .4, ki = 1$ and $T_L = 10$. (a)$k = 0.17$,(b)$k = 0.18$.

and $T_L = 0.5$, a continuation method permits to obtain the evolution of x_1 versus the values of k (see figure 7). Three singularities are obtained on such curve: two Hopf bifurcation points (N_s)and a limit point F(Saddle-node bifurcation or Fold). The Saddle-node bifurcation possesses has one of its eigenvalue equal to zero and the following coordinates in phase space :
$(x_{10}, x_{20}, x_{30}, x_{40}) = (0.345, -0.219, 0, 0.817)$
and the corresponding eigenvalues are:
(-4.066+i12.01,-4.066-i12.01,-0.008,-4.736e-005).
The two neutral saddles have the following coordinates:
$(x_{10}, x_{20}, x_{30}, x_{40})$ =(0.356, -0.233, 0, 0.751) with the associates eigenvalues:
(-4.072 + i11.079,-4.071 -i11.079, -0.179, 0.179) and $(x_{10}, x_{20}, x_{30}, x_{40})$ =(0.431,-0.353, 0, 0.343) with the eigenvalues (-4.065 + i6.629,-4.066 -i6.629, -0.573, 0.573). The three singularities detected in this section are to be used as starting points to trace the bifurcation curves in a two parameter plane chosen here as (k,T_L)-plane depending mainly on the rotor resistor and the rotor time constant.

5.3 Cusp point and Bogdanov-Taken bifurcation

The continuation of the limit point (LP) detected in previous section leads to trace a saddle-node bifurcation curve shown in figure 8, such curve includes two branches joining in a codimension two bifurcation point, namely cuspidal point (CP) having the following phase space coordinates:

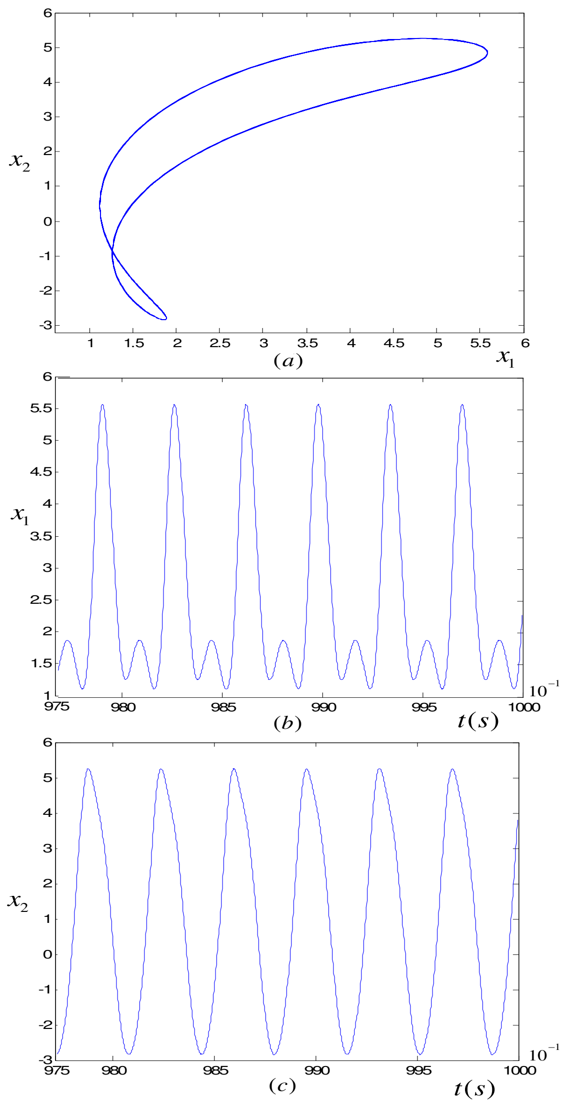

Figure 6: Oscillatory phenomenon: (a) phase trajectory in phase planes (x_1, x_2) (b) direct flux waveform (c) quadratic flux waveform

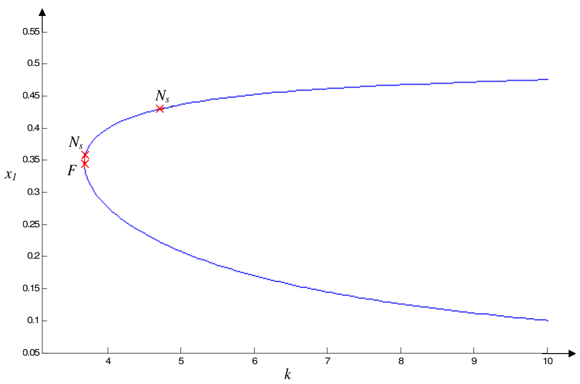

Figure 7: Limit point and Neutral Saddle Points

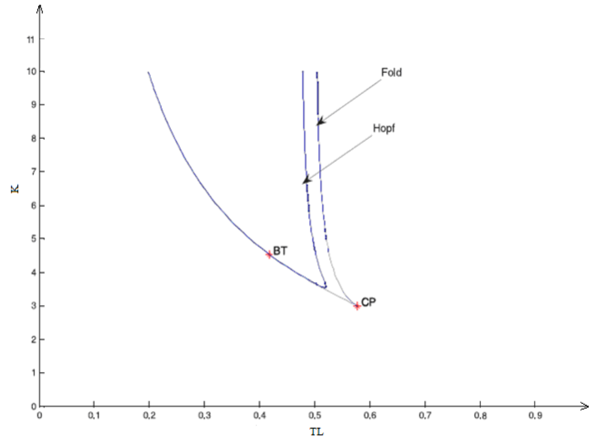

Figure 8: Fold and Hopf bifurcation curves in (k, T_L)-plane

$(x_{10}, x_{20}, x_{30}, x_{40}) = (0.5, -0.289, 0, 0.578)$. Besides, such curve presents another codimension two bifurcation in $(x_{10}, x_{20}, x_{30}, x_{40}) = (0.266, -0.182, 0, 0.891)$, having two eigenvalues equals to zero and known as Bogdanov-Taken bifurcation (BT). Then, using the Hopf bifurcation points , met in the same continuation path of the equilibrium point as the limit point (LP) in previous section, we obtain the Hopf bifurcation curve in (k, T_L)-plane, which is seemingly enclosed in the saddle-node bifurcation curve as in figure 8. the left branches of the two different bifurcation curves seem to be merged together but they are not so, several 'zooms' of this part permits to realize that there is no intersections between such bifurcation curves, so that the Hopf bifurcation curve is completely contained inside the quasi-lip structure. Varying rotor time constant T_L from 0. to 1.1, the continuation of an equilibrium point $(x_{10}^*, x_{20}^*, x_{30}^*, x_{40}^*) = (0.7236, -0.3618, 0, 0.191)$ computed for the parameters $k = 4, kp = .4, ki = 1$ and $T_L = 0.5$ is illustrated by figure 9. Such curve includes two limit points F_1 and F_2 and two Hopf bifurcation points H_1 and H_2, these bifurcation points lead to the same results obtained above and illustrate the fact that the two saddle-node bifurcation are the junction of three different sheets, and the Hopf bifurcation is located on the inner sheet between the upper and the lower ones.

5.4 Bifurcation scenario for PI controller parameters

After the discussion of the effect of real parameter machine k, in this subsection we aim to study the influence of the PI controller parameters k_i

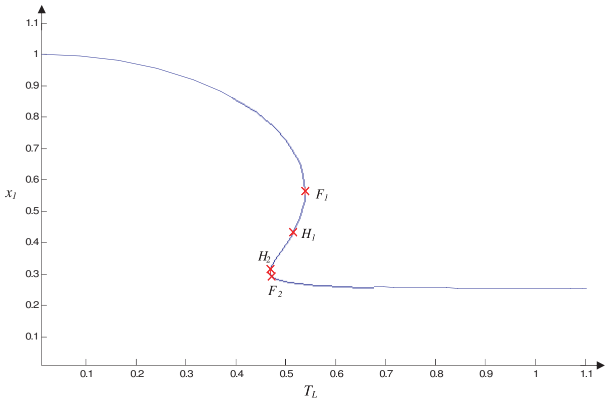

Figure 9: Limit points and Hopf bifurcation

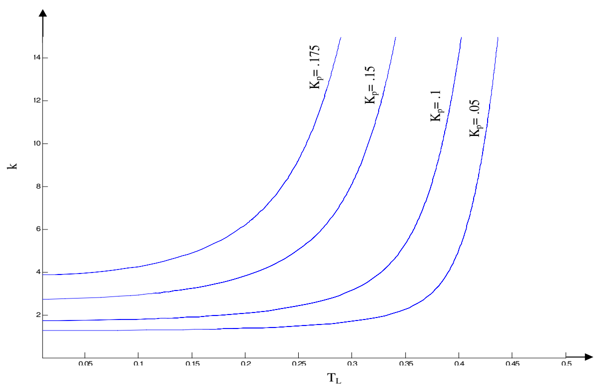

Figure 10: values of k corresponding to a Hopf bifurcation. T_L for different values of k_p

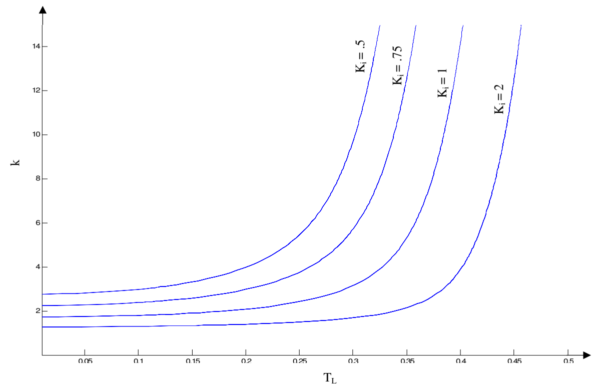

Figure 11: values of k corresponding to a Hopf bifurcation vs. T_L for different values of k_i

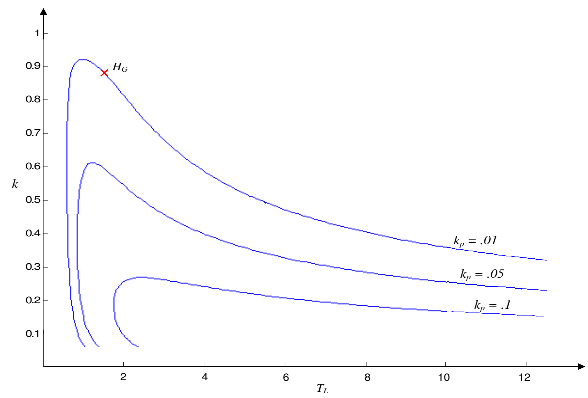

Figure 12: values of k corresponding to a Hopf bifurcation vs. T_L for different values of k_p and for larger values of T_L

and k_p on the bifurcation structure in the (k,T_L)-parameter plane. Similar to the previous discussion, we will discuss the appearance of Hopf bifurcation. Thus, a set of Hopf bifurcation curves are traced for a small range of load torque values T_L in figure 10 for different values of k_p. These bifurcation curves were obtained for ($k_i = 1$). For the same range of load torque, a second set of bifurcation curves obtained for fixed ($k_p = 0.1$) and for certain values of (k_i) is given in figure 11. For a larger range of load torque values, another set of Hopf bifurcation curves with different shapes presenting an extremum computed for different values of k_p in the same parameter plane (k,T_L) see figure 12. In figure 13, we trace the Hopf bifurcation in (k_p, k_i)-plane for T_L=2.5-5.5-7.5 and 10. In both cases of T_L=7.5 and T_L=10 a codimension two bifurcation point, namely a Generalized Hopf bifurcation is identified. Such bifurcation is a control bifurcation because it depends on PI controller parameters k_p and k_i.

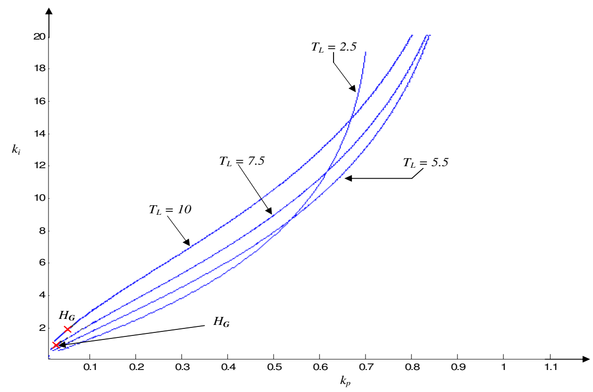

Figure 13: Generalized Hopf bifurcation curves

6 Features of the transition to chaos

Aiming to investigate the complex chaotic phenomena in the studied model, this section presents some graphical results that illustrate the under-

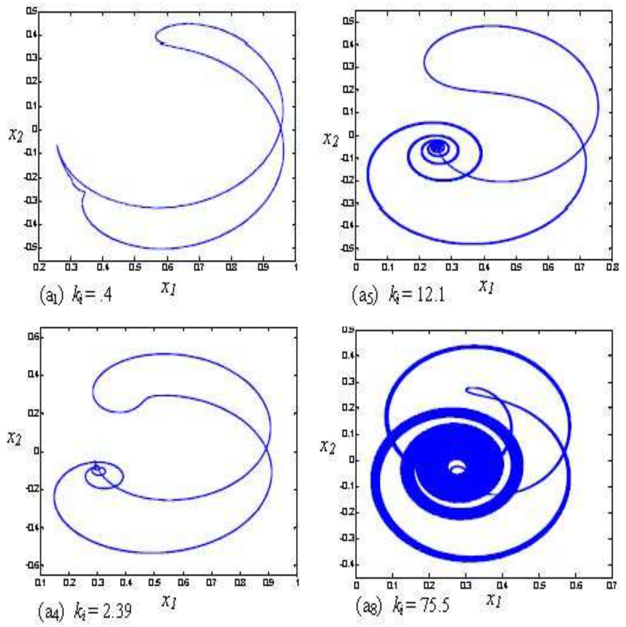

Figure 14: Transition Hopf bifurcation-chaotic behavior

lying mechanism of the chaos generation. The first case of the chaos detection is shown through a transition Hopf bifurcation-chaotic attractor. The variation of ki parameter from 0.21 to 120, shows the appearance of equilibrium points which undergoes a Hopf bifurcation in the ki-interval $[0.22, 0.3]$ giving rise to a limit cycle. The phase portraits of the limit cycles present a cuspidal point around which an oscillating part of the trajectory is as important as ki increases. we recall that according to previous studies [19], this phenomenon was related to the important role of higher harmonics whose amplitudes become as more important as the number of modulations is great. But the main result to be emphasized here is that the increasing oscillations around the phase trajectory cuspidal point leads to a chaotic behavior as shown in figure 14. The nature of the possible bifurcations that may occur in ki-interval [0.3, 75.5],and which exhibit the qualitative change seemingly spectral change of behaviors needs to be deeply investigated. The figure 14 was obtained for the same initial conditions set $(x10, x20, x30, x40) = (0.07, 0.152, 0.953, 0.71)$, for the parameter values $k = 4$, $k_p = .01$, $T_L = .5$ and for different values of k_i. In addition, a transition from a simple oscillatory phenomenon (limit cycle) to complex oscillatory phenomenon (chaos) is identified according to the Generalized Hopf bifurcation occurrence. Indeed, before the GH bifurcation detection, the system exhibits a limit

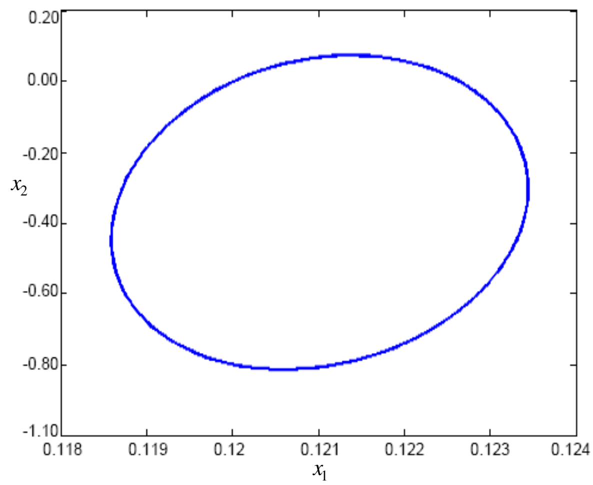

Figure 15: Limit cycle generated before Generalized-Hopf detection

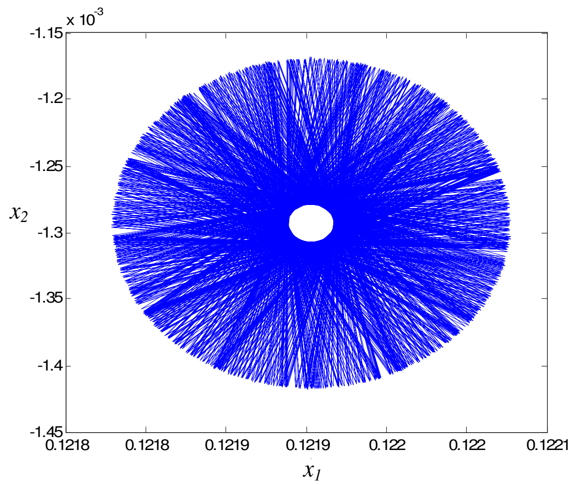

Figure 16: Chaotic torus state generated at Generalized-Hopf

cycle (see figure 15) for the parameter set of a Hof bifurcation $k = 7.91$, $k_i = 2.225$, $k_p = 0.084$, $\tau_L = 10$ and with the associates eigenvalues [-2.4-3.52e+002i; -2.4+3.52e+002i; -0.0011 - 0.677i; -0.0012 + 0.676i]. Whereas, after the GH bifurcation occurrence the oscillation of the system responses became more complex and the figure 16 shows a chaotic torus generated by model equations with parameter setting $k = 8.203$, $k_i = 1.675$, $k_p = 0.025$, $\tau_L = 10$ and for the initial conditions set $(x_{10}, x_{20}, x_{30}, x_{40})$=$(1, 0.152, 0.3, 0.1)$.

This case presents a class of chaotic attractors with spherical patterns, where the computed attractor looks like torus. The occurrence of this chaotic state is detected near the codimension 2 Generalized-Hopf (GH) bifurcation point witch is a bifurcation of an equilibrium point at which the generated critical point has one pair of purely imaginary eigenvalues [-4.0-2.716e+003i;-4.0+2.7160e+003i;-0.0091- 0.351i ; -0.0091 + 0.351i] and the first lyapunov coefficient is equal to zero. Therefore, this bifurcation can imply a local birth of chaotic behavior.

7 Conclusion

This paper reviews a numerical study of the dynamic behavior of an IFOC induction motor where a PI controller takes place, with particular reference to bifurcation analysis. Specifically, we have investigated how the PI controller parameters influence the bifurcation sets. Computational techniques are applied to calculate the steady states and to delineate the bifurcation curves wich separate the regions of qualitatively different behaviors. Based on the obtained numerical results and graphical simulations, we have shown the existence of regular behavior and region where chaotic phenomena may occur depending on a small variation of both motor parameters (k, T_L) and PI controller gains. The occurrence of chaotic phenomena is detected for particular values of k_p and k_i. Two features of the transition to chaos are presented. Such analysis provide useful guidelines for the setting of tunable motor parameters and to practically adjust the PI controller gains.

Acknowledgment

This work was supported in part by RME: Electrical Machines and Power Systems Unit of Research, INSAT-Tunisia. Professor Rachid Dhifaoui is the Director of RME Unit.

References:

[1] Mira .C, J. P. Carcassès , C. Simo and J. C. Tatjer. Crossroad area-spring area transition. (II) Foliated parametric representation, *International Journal of Bifurcation and Chaos*, 1(2), pp. 339-348, 1991.

[2] Nizar Jabli, Hedi Khammari and Mohammed Faouzi Mimouni, Chaos-low periodic orbits transition in a synchronous switched circuit, WSEAS Transactions on Circuits and Systems Issue 12, Volume 7, December 2008.

[3] Duran. M.J, Salas. F and Arahal. M.R, Bifurcation Analysis of Five-Phase Induction Motor Drives With Third Harmonic Injection, *IEEE Transactions on Industrial Electronics*, Volume 55, Issue 5, pp. 2006 - 2014, 2008.

[4] Yongyao Lu, Hongmei Li and Wensheng Li, Hopf bifurcation and its control in an induction motor system with indirect field oriented control, *4th IEEE Conference on Industrial Electronics and Applications (ICIEA'2009)*, pp. 3438 - 3441, 2009.

[5] Kanwarjit Singh Sandhu and Vineet Chaudhary, Simulations of Three- Phase Induction Motor Operating with Voltage Unbalance. Proceedings of the 8th WSEAS International Conference on Electric Power Systems, Higher Voltage Electric Machines, POWER '08. Venice, Italy, November 21-23, 2008.

[6] Seok Ho Jeon, Dane Baang and Jin Young Choi, Adaptive Feedback Linearization Control Based on Airgap Flux Model for Induction Motors, *International Journal of Control, Automation, and Systems*, vol. 4, no. 4, pp. 414-427, 2006.

[7] Bazanella A.S. and R. Reginatto, Instability Mechanisms in Indirect Field Oriented Control Drives: Theory and Experimental Results, *IFAC 15th Triennial World Congress, Barcelona, Spain,*, 2002.

[8] Bazanella A.S., R. Reginatto and R.Valiatil, On Hopf bifurcations in indirect field oriented control of induction motors: Designing a robust PI controller, ***1**, Proceedings of the* 38th *Conference on Decision and Control, Phoenix, Arizona USA.*, 1999.

[9] Reginatto .R, F. Salas, F. Gordillo and J. Aracil, Zero-Hopf Bifurcation in Indirect Field Oriented Control of Induction Motors, *First IFAC Conference on Analysis and Control of Chaotic Systems (CHAOS'06)*, 2006.

[10] Salas .F, R. Reginatto, F. Gordillo and J. Aracil, Bogdanov-Takens Bifurcation in Indirect Field Oriented Control of Induction Motor Drives, *43rd IEEE Conference on Decision and Control*, Bahamas, 2004.

[11] Salas .F, F. Gordillo, J. Aracil and R. Reginatto, Codimension-two Bifurcations In Indirect Field Oriented Control of Induction Motor Drives, *International Journal of Bifurcation and Chaos*, **18**(3), pp. 779-792, 2008.

[12] de-Wit .C.C, J. Aracil, F. Gordillo and F. Salas, The Oscillations Killer: a Mechanism to Eliminate Undesired Limit Cycles in Nonlinear Systems, *(CDC-ECC'05)*, Seville, Spain, 2005.

[13] Zhang .B, Y. Lu and Z. Mao, Bifurcations and chaos in indirect field-oriented control of induction motors, *Journal of Control Theory and Applications*, **2**, pp. 353-357, 2004.

[14] Algaba .A, E. Freire, E. Gamero and A. J. Rodriguez-Luis, Analysis of Hopf and Takens Bogdanov-Bifurcations in a Modified van der Pol-Duffing Oscillator, *Nonlinear Dynamics*, 16 pp. 369-404, 1998.

[15] Bazanella .A.S and R. Reginatto, Robustness Margins for Indirect Field-Oriented Control of Induction Motors, *IEEE Transaction on Automatic Control*, **45**, pp. 1226-1231, 2000.

[16] N. Jabli, H. Khammari, M.F. Mimouni, Bifurcation scenario and chaos detection under variation of PI controller and induction motor parameters. Proceedings of the 9^{th} WSEAS International Conference on Non-Linear Analysis, Non-Linear System and Chaos (NOLASC '10), Sousse, Tunisia, 3 - 6 Mai 2010.

[17] Gordillo .F, F. Salas, R. Ortega and J. Aracil, 2002. Hopf Bifurcation in indirect field-oriented control of induction motors, *Automatica*, **38**, pp. 829-835.

[18] N. Jabli, H. Khammari, M.F. Mimouni, An analytical study of bifurcation and nonlinear behavior of indirect filed-oriented control induction motor. Proceedings of the 6^{th} WSEAS International Conference on dynamical systems & control (CONTROL'10) Sousse, May 3-6, 2010.

[19] Khammari .H, C. Mira and J.P. Carcasses, 2005. behavior of harmonics generated by a Duffing type equation with a nonlinear damping, Part I. International Journal of Bifurcation and Chaos, Vol. 15, No. 10, pp. 3181-3221.

[20] Lan Xu, Beimei Chen, Yun Zhao and Yongluo Cao, 2008. Normal Lyapunov exponents and asymptotically stable attractors, Dynamical Systems, Volume 23, Issue , pp. 207 - 218.

Nizar Jabli was born in Gafsa in 1977, Tunisia. He received the Engineer Diplomat and Master's degree from National Engineering School of Sfax and Monastir, Tunisia, respectively, in 2003 and 2005. He is currently working toward the PhD degree at Monastir University, Tunisia. His research interests are in the area of electric systems and circuits control: bifurcation and chaos theory. Mr. Jabli is Member, IEEE and RME Unit of Research.

Hedi Khammari was born in Kairouan, Tunisia in 1963. He received the engineer diploma and the Master degree from National Engineering School of Tunis in 1988 and 1990 respectively. He received PhD in Electrical Engineering in 1999. His research interests are mainly in the area of nonlinear dynamics and the application of chaos theory in different fields namely communication, electric systems and bioinformatics.

Mohamed Faouzi Mimouni was born in Siliana, Tunisia in 1960. He received PhD in Electrical Engineering in 1997. He is currently Professor at National Engineering School of Monastir, Monastir University, Tunisia. His research interests are electric machine control and power systems. Professor Mimouni is Member in RME Unit of Research.

Rachid Dhifaoui was born in Kairouan, Tunisia in 1954. He received PhD in Electrical Engineering from ENSET, University of Tunis II, in 1991. He is currently Professor at National Institute of Applied Sciences and Technology. He manages the studies of a Master Cycle in Industrial Informatics and Automatic Control. His research interests include Power Systems and Electric Machines and Networks. Professor Dhifaoui is also the Director of RME Unit of Research.